https://doi.org/10.22226/2410-3535-2022-4-321-326

Experimental and theoretical study of the conditions for the formation of carbon nanostructures in an arc discharge in helium, argon and nitrogen

S. Sakhapov[†,1], V. Andryushchenko[1], E. Boyko[1], M. Skirda[1], D. Smovzh[1,2]

[†]sakhapov@gmail.com

[1]Kutateladze Institute of Thermophysics, Novosibirsk, 630090, Russia
[2]Novosibirsk State University, Novosibirsk, 630090, Russia

Experimental measurements and numerical simulation of plasma parameters of an electric arc discharge in helium, argon, and nitrogen media at pressures of 25 Torr were carried out. On the basis of a theoretical model and experimental data on the interelectrode distance and the rate of sputtering of the anode, the radial distribution of the gas temperature is calculated. The obtained distribution is consistent with measurements carried out using a probe with a thermocouple, and the residence times of the sputtered material in different temperature ranges are determined. The properties and morphology of soot synthesized on the chamber walls were investigated by HRTEM, XRD and TGA methods. It is shown that during an arc discharge in nitrogen, the maximum number of graphite structures arises as a result of a longer residence of the sputtered carbon particles arising in the process at temperatures of about 700 –1700°C.

Keywords: arc discharge, sputtering, graphite, carbon materials, helium, argon, nitrogen.

1. Introduction

The overwhelming majority of modern new materials contain carbon in various allotropic modifications. Fullerenes, carbon nanotubes and graphene materials are actively used as modifying additives in various applications related to catalysis [1], electrochemistry [2], medicine [3], etc. In parallel with the development of composite materials applications using carbon nanostructures, methods of their production are being actively developed. The arc discharge can be considered as the basic technology for the synthesis of all currently existing carbon nanomaterials. The main disadvantage of the arc discharge is the low selectivity of the synthesis: for instance, the maximum concentration of fullerenes in soot obtained during the synthesis by the arc discharge was only 25% [4]. The concentration of carbon nanotubes (CNTs) obtained by arc discharge synthesis can reach 75% [5]. This is due to the high gradients of parameters during arc discharge synthesis. The characteristic growth times are shorter than the times for establishing thermodynamic equilibrium, which leads to the formation of a wide range of reaction products from amorphous carbon to graphite [6]. Theoretical approaches for describing processes in an arc were developed by Iijima S. [7], Keidar M. et al. [8,9], Alekseyev N.I. and Dyuzhev G.A. [10–13] and others. Attempts have been made to describe the kinetics of electrode evaporation, product condensation, and the structure of flows in the reactor for various arc discharge modes. However, at the moment there is no theoretical model capable of describing the processes of electric arc sputtering, which is associated with a large number of interrelated parameters affecting the processes, and insufficient understanding of the mechanisms of sputtering and condensation in the arc.

Arc discharge synthesis is inferior to the combustion method in terms of mass synthesis of fullerenes [14]. For the synthesis of CNTs, CVD methods having significantly better synthesis selectivity are more efficient. Nevertheless, an electric arc discharge can be used if it is necessary to synthesize high quality CNTs [15]. Another interesting application of arc discharge is the synthesis of metal-carbon composites for catalytic and electrochemical applications [16]. In this case, requirements are imposed both on the structure and composition of nanoparticles and on the carbon matrix in which they are dispersed. By changing the synthesis conditions, it is possible to change the concentration of carbon in the nanoparticles of the additive and their phase state [17]. At the same time, electrochemical applications require sufficient electrical conductivity of soot, which can be achieved by increasing the concentration of graphite-like nanostructures in it: for instance, CNTs or graphene [18]. Unlike CNTs and fullerenes, the yield of graphene during arc synthesis can be much higher. For instance, technologies for cheap and efficient electric arc synthesis of graphene were demonstrated in the articles [19,20]. The most effective way to increase the graphene concentration in sputtering products is to use specified buffer mixtures during sputtering. At the same time, two mechanisms of the influence of the buffer gas are discussed in the scientific literature. The first is associated with the participation of buffer gas molecules in chemical transformations during the growth of carbon nanostructures;

this mechanism is typical for atmospheres containing oxygen and hydrogen [19 – 23]. The second mechanism is associated with a change in the kinetics of condensation of materials due to different cooling rates determined by the pressure of the buffer gas or its thermal conductivity [24 – 26]. In the case of using chemically inert mixtures, in addition to changing the heat transfer parameters associated with different thermal conductivity of the gas, the discharge parameters change, which leads to a change in the plasma temperature and mass fluxes due to a change in the evaporation rate of the electrodes [24]. The structure of soot formed during electric arc sputtering is determined by the kinetics of cooling materials at the stage of formation of soot nuclei with a closed structure such as fullerenes [27] or flat particles [28] and subsequent condensation of the bulk of carbon at a lower temperature.

The aim of this study is to develop an electric arc method for the synthesis of composite materials with a given degree of graphitization of the carbon matrix. The electric arc sputtering modes and the structure of the forming carbon material are experimentally investigated.

2. Materials and methods

The study of the arc discharge was carried out in a sealed chamber (1), shown in Fig. 1, which was evacuated by a foreline pump to pressures less than 0.05 Torr before the experiments. The chamber was filled with buffer gases (He, Ar, N_2) up to a pressure of 25 Torr. The electrodes were graphite rods 8 mm in diameter, positioned so that the chamber symmetry axis coincided with the axes of the electrodes. A grounded cathode 2 cm long (2) was attached from above to a fixed holder. An anode 6 cm long was attached to the insulated input (3), to which a positive voltage was applied from a high-voltage power source so that the discharge current was 100 A. The voltage at the discharge was automatically maintained at a constant level throughout the experiment by moving the evaporating anode. The temperature distribution along the radius was measured by a movable probe (4), at the end of which a chromel-alumel thermocouple was attached. The vacuum chamber, electrode attachments, and vacuum inlets were cooled by a water flow through the channels located inside them.

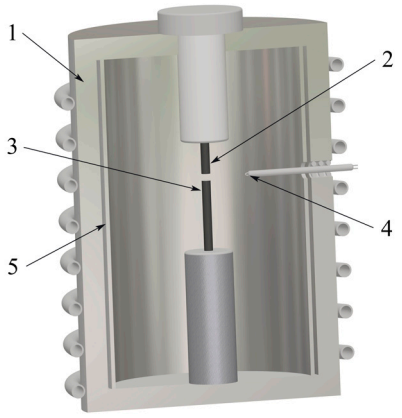

Fig. 1. The experimental setup (1 — chamber, 2 — graphite cathode, 3 — graphite anode, 4 — movable probe, 5 — removable stainless steel shell).

During the experiments, the anode was sputtered, which led to the appearance of carbon vapors in the near-arc region. Diffusion of carbon particles from the arc discharge plasma zone to the chamber walls led to their mixing with the surrounding gas, cooling and condensation into larger formations, which were deposited on the chamber walls. To simplify the collection of soot, the chamber walls were closed from the inside with a re-movable stainless steel shell (5).

To describe the dynamics of propagation of a fan jet with a heterogeneous composition, which is formed during electric arc sputtering of an electrode in an arc discharge in a buffer gas atmosphere, it is necessary to create a theoretical model that describes the main phenomena occurring in the system. In this work, the model for calculating electric arc sputtering proposed by Keidar [8, 9] is modified to calculate the kinetics of carbon vapor condensation during electric arc evaporation in atmospheres of chemically inert gases. The model consists of five main parts: the processes occurring in the arc, anode evaporation, jet propagation, transfer of atoms by the jet and their ionization. Let us briefly consider the basic equations and the corresponding boundary conditions.

To find the current density, Eq. (1) is solved for the electrical conductivity σ and the electrical potential φ:

$$\nabla \cdot \left(-\sigma \nabla \varphi\right) = 0. \qquad (1)$$

The potential of a weakly ionized plasma in a direct current field is found according to the Chapman-Enskog equation:

$$\sigma = \frac{e^2}{m_e} \frac{n_e}{\left(\nu_{e,a} + \nu_{e,i}\right)},$$

where e, m_e, n_e is the charge, mass and concentration of electrons, respectively, and $\nu_{e,a}$, $\nu_{e,i}$ are the frequencies of collisions of electrons with neutral atoms. The latter are determined according to the following equations:

$$\nu_{e,a} = \frac{4}{3}\left(\frac{8k_B T}{\pi m_e}\right)^{1/2} n_a Q_m$$

and

$$\nu_{e,i} = \frac{4\sqrt{2\pi}}{3} n_i \left(\frac{e^2}{k_B T}\right)^2 \left(\frac{k_B T}{m_e}\right)^{1/2} \ln\left(\Lambda\right),$$

where n_a, n_i are the concentrations of neutral atoms and ions, Q_m is the cross section for collisions of electrons with neutral atoms, ln(Λ) is the Coulomb logarithm for plasma.

To determine the axially symmetric magnetic field, Ampere's law is used:

$$B_\theta = \frac{\mu_0}{r} \int_0^R j_z r dr, \qquad (2)$$

where R is the experimental cell radius. It is assumed that the plasma under study is in local thermodynamic equilibrium, therefore, to determine the degree of ionization of particles, using the Saha equation.

To simulate the flow propagation, the standard continuity equation is used, as well as the Navier-Stokes equations,

taking into account the presence of a gravity field and an electromagnetic field:

$$\frac{\partial(\rho\vec{u})}{\partial t}+\nabla\cdot(\rho\vec{u}\vec{u})=-\nabla p+\nabla\cdot(\mu\vec{u})+\rho\vec{g}+\vec{j}\times\vec{B}.$$

To find the temperature distribution, the equation for heat transfer in enthalpy form is solved, which takes into account the Joule heat and the heat flux of electrons:

$$\frac{\partial(\rho h)}{\partial t}+\nabla\cdot(\rho\vec{u}h)=\frac{Dp}{Dt}+\nabla\cdot\left(k\nabla\left(\frac{h}{C_{p,m}}\right)\right)+$$
$$+\frac{\vec{j}\cdot\vec{j}}{\sigma}+\frac{5}{2}\frac{k_B}{e}\vec{j}\cdot\nabla\left(\frac{h}{C_{p,m}}\right).$$

To determine the position of the evaporated particles in space, the standard diffusion equation is used:

$$\frac{\partial(\rho c)}{\partial t}+\nabla\cdot\left(\rho\vec{u}c\right)=\nabla\cdot\left(D\nabla(\rho c)\right),$$

where c is the mass fraction of atoms and D is the diffusion coefficient.

The computational domain is a cylindrical cell with two electrodes of the same diameter. The axes of the electrodes and the cylindrical cell are collinear. The potential of the electric field at the end of the cathode and the current density at the end of the anode are considered constant. On all other surfaces, the current density is zero. The flow rates are assumed to be zero on all surfaces except the end of the anode. The anode evaporation rate and the interelectrode distances were set directly from the experiment. The mass velocity of the sublimated vapor at the end of the anode is obtained by dividing the mass flow rate of evaporation (taken from the experiment) by the sum of the vapor density and the local density of the liquid, near the interface. The wall temperature of the computational domain is considered constant and equal to 80°C. Heat fluxes are set at the ends of the electrodes. To solve the diffusion equation, the particle flux at the end of the anode is used; the remaining surfaces of the computational domain are considered impenetrable.

3. Results and discussion

The electrode was sputtered in an arc discharge in helium at various pressures. During the arc discharge, the radial distribution of the gas temperature was measured using a thermocouple probe moved from the chamber walls to the center. The probe was located at the level of the gap between the anode and cathode. The radial temperature distribution measured by the probe method for various gases in the discharge chamber is shown in Fig. 2a (markers). Experimental data on discharge parameters (distance between electrodes, anode sputtering rate, and the rate of soot deposition on the removable stainless steel shell) of the arc discharge are shown in Fig. 2b.

The synthesized material, which is soot, was collected from a cooled removable shell of the vacuum chamber and studied by XRD, TGA, HRTEM. The thermogravimetric analysis (TGA) results of the synthesized carbon black, performed in a He:O_2 mixture (80:20) at a rate of 10 degrees per minute, are shown in Fig. 3a. According to the TGA, the soot obtained in a discharge in He completely burned out at a temperature of 850°C, while in the soot formed in N_2 and Ar about 1 and 3% of the initial mass remains, respectively. The results of derivative thermogravimetric (DTG) and differential scanning calorimetry (DSC) analyzes are shown in Fig. 3b. The synthesized material begins to burn intensively after 300°C: according to DSC analysis, an exothermic process occurs with peaks at 522°C in N_2, and 510°C for soot synthesized in He and Ar. Incomplete burnout of carbon materials in N_2 and Ar is explained by the presence of thermally stable carbon phases in them.

The results of the study of the samples by the XRD method are shown in Fig. 4. According to these data, the most graphitized soot was synthesized in a nitrogen discharge and had a coherent scattering region (CSR) size equal to 22 nm. There are significantly less graphite structures in the material synthesized in an arc discharge in argon than in nitrogen, and small peaks characteristic of fullerene phases 111, 220, and 311 appear.

The difference in the morphology of the soot synthesized in the arc discharge in different buffer gases can be observed

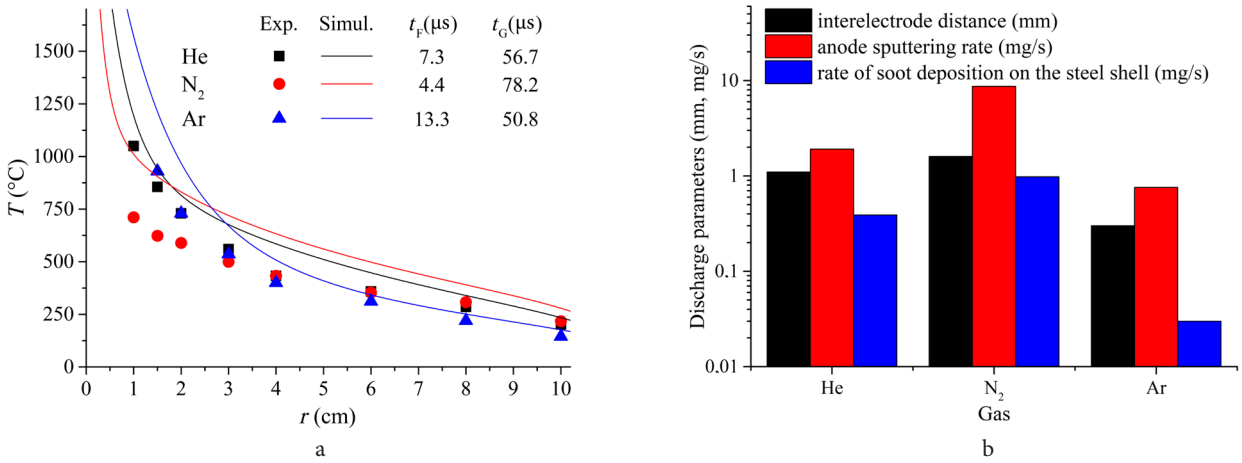

Fig. 2. (Color online) Experimental (markers) and theoretical (lines) radial distributions of gas temperature from the distance to the center of the arc discharge in helium, nitrogen and argon. The residence times of particles in the temperature range from 1700 to 2500°C – t_F and 1700 – 700°C – t_G (a); Experimental data on discharge parameters (b).

in the HRTEM images shown in Fig. 5,6 a,b for helium, nitrogen and argon, respectively. These figures also show the areas with crystal lattices that were processed using the Fast Fourier transform (FFT). The reflections on the FFT correspond to the crystal lattice planes of graphite with a hexagonal crystal structure of the space group P63/mmc [JCPDS Card No. 00-041-1487].

The material produced in the arc discharge consists mainly of amorphous carbon. The material synthesized as a result of an arc discharge in nitrogen is amorphous carbon with a large number of graphite structures, including closed ones, as can be seen in Fig. 6 a. The formation of fullerene-like structures is observed in soot when sputtered in all buffer gases (Fig. 6 b), however, graphite crystallites are rare. HRTEM images (Fig. 5) of a carbon material formed as a result of sputtering a graphite anode in an arc discharge in a helium medium did not show the presence of graphite structures, which can be explained by their small number and locality of HRTEM measurements. However, the presence of graphite is confirmed by XRD measurements, confirming the presence of a small amount of graphite crystallites (Fig. 4).

The calculated dependence of the gas temperature on the distance to the center of the arc discharge is additionally shown as lines in Fig. 2 a together with the experimental data. It can be seen that the experimental data are in qualitative agreement with the calculation. The weaker temperature gradient in the initial section for sputtering in argon is associated with the lower thermal conductivity of this gas in comparison with nitrogen and helium. The noticeable difference between the theoretically calculated temperature distribution and experimental measurements in nitrogen is explained by the fact that the internal structure of molecules is not taken into account in the calculation algorithm. For a diatomic nitrogen molecule, part of the energy is spent on the excitation of one vibrational and two rotational degrees of freedom. In this case, the greatest deviations of the simulation and experimental data are observed at high temperatures. This was to be expected, since the excitation temperature of the vibrational degree of freedom for the nitrogen molecule is on the order of 3700°C.

The temperature gradient determines the characteristic residence times of the forming carbon nanoparticles in the

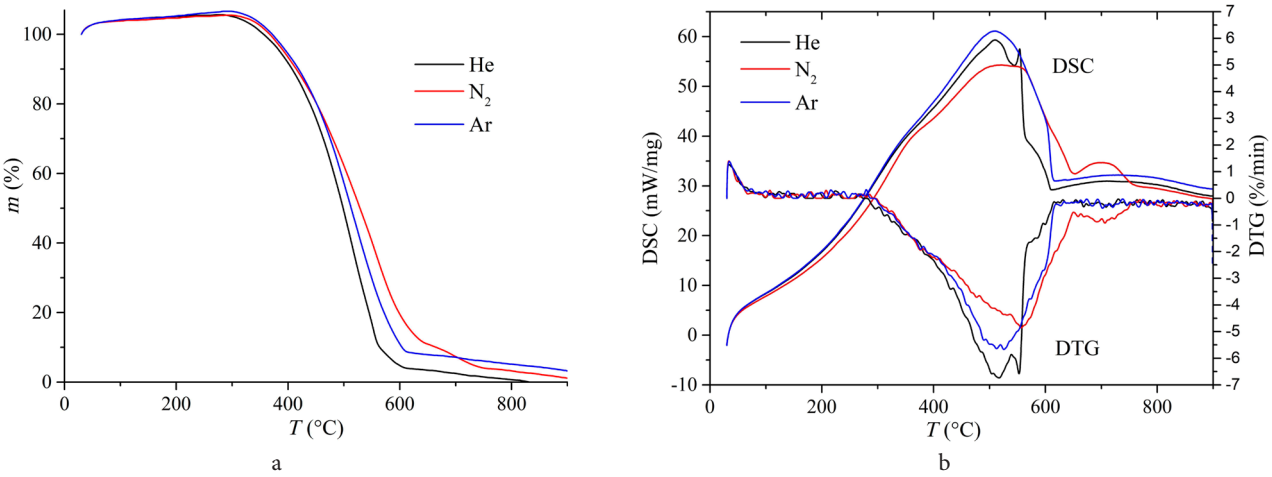

Fig. 3. (Color online) Thermogravimetric analysis (a); derivative thermogravimetric (DTG) and differential scanning calorimetry (DSC) analysis of materials synthesized in an arc discharge in He, N_2 and Ar atmospheres (b).

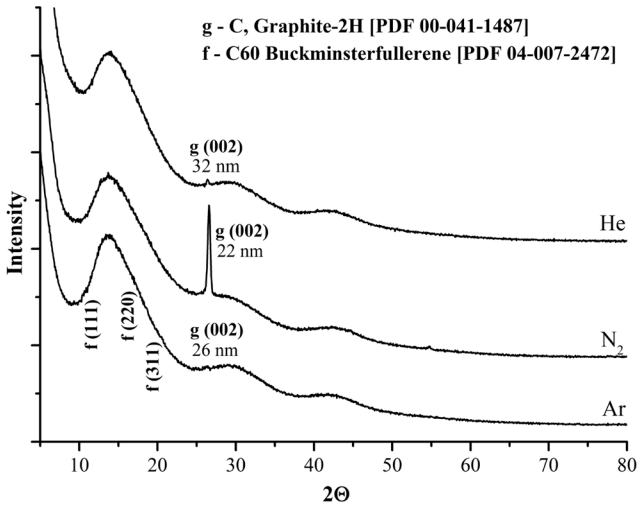

Fig. 4. X-ray diffraction patterns of materials synthesized in an arc discharge in He, N_2 and Ar atmospheres and CSR sizes for the corresponding peak.

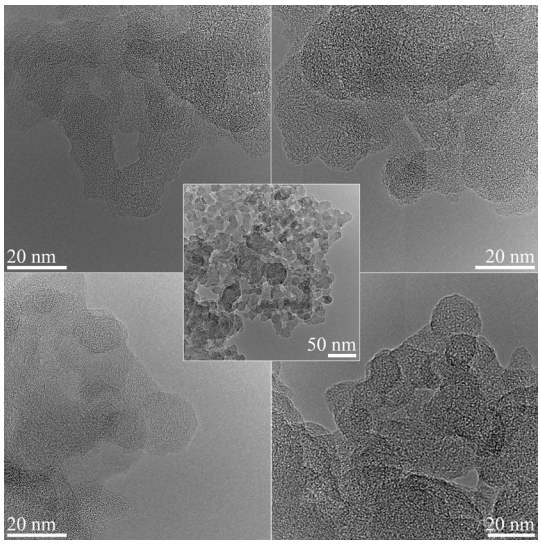

Fig. 5. HRTEM images of soot synthesized in an arc discharge in helium.

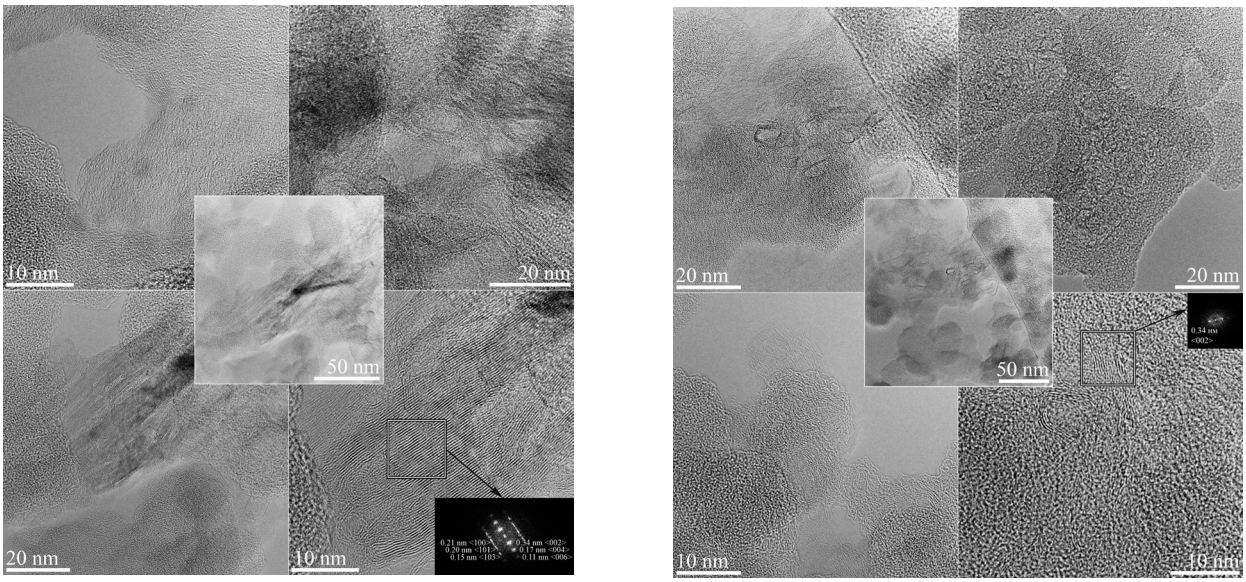

a b

Fig. 6. HRTEM images of soot synthesized in an arc discharge: in nitrogen (a); argon (b).

zones corresponding to the formation of various allotropic modifications of carbon. In modern models of the formation of soot during arc sputtering, it is assumed that the structure of soot is determined by the shape of the nuclei growing at the initial stage of condensation. The fullerene model assumes that a spherical molecule (fullerene) is the nucleus of a soot globule. The kinetics of soot formation can be changed: for instance, in [20, 21] it is shown that the addition of hydrogen slows down the formation of closed structures and leads to the formation of graphene layers. A similar effect is achieved by increasing the cooling rate of materials [26]. The cooling rate depends on the thermal conductivity of the buffer gas, which under the conditions of our experiments is maximum for helium and minimum for argon. But for nitrogen, the material flow rate is significantly higher, which leads to faster material quenching at high temperatures. The temperature range of fullerene formation is assumed to be from 1700 to 2500°C [29 – 31], the residence time of vapors at a given temperature (t_F) for nitrogen is 1.7 times less. The sputtering rate of the electrodes, in turn, depends on the discharge parameters, plasma temperature, current-voltage characteristics, which are determined by the type of buffer gas. Thus, the kinetics of vapor cooling depends not only on the thermal conductivity of the buffer gas. Further, in the process of vapor cooling, the effect of the difference in flow rates weakens, and at low velocities the main contribution to the kinetics is made by the gas thermal conductivity, Fig. 2b. Thus, for nitrogen, the residence time in the hot zone of nucleation formation is significantly reduced and the residence time in the growth region of graphite structures increases (temperature range 1700 – 700°C – t_G). This leads to the fact that at the initial stage of growth, the nuclei do not have time to curl up and have planar symmetry, and subsequently, the material is in the phase of active growth of graphene layers for a longer time, and, accordingly, the material graphitization degree and the scale of graphite regions increase.

4. Conclusions

Simulation of the homogeneous fan-shaped jet propagation arising in an arc dis-charge has been carried out. For the simulation, a self-consistent physical model of the arc discharge was used, which includes the calculation of the ionization and plasma potential, the propagation of the gas flow from the plasma zone to the surrounding buffer gas, and the synthesized particles spatial distribution. Experimental data on the density of the rate of sublimation from the anode surface and the distance between the anode and the cathode were taken as known values. The calculated dependence of the gas temperature on the distance to the arc center is in good agreement with the experimental data obtained using a thermocouple probe.

The morphology and structure of the soot formed on the walls of the chamber were investigated. The synthesized material mainly consists of amorphous carbon with graphite crystallites, the maximum amount of which is formed during an arc discharge in nitrogen, which agrees with the calculated data on the residence time of particles in the gas flow in the temperature range from 700°C to 1700°C. As a result, it was shown that one of the main factors affecting the composition of the resulting soot is the residence time of carbon in certain temperature ranges, which is determined by the thermal conductivity of the buffer gas and the parameters of the arc discharge. This information will be useful in the design of installations for the synthesis of carbon-containing materials and the selection of their operating mode.

Acknowledgment. Work on the manufacturing of an arc discharge installation, materials synthesis and measurements by TEM, XRD and numerical calculations were supported by the Russian Science Foundation, project No. 18-19-00213. Measurement by TGA were carried out with the support of state contract IT SB RAS No. 122020200256-6. The authors acknowledge shared research facilities VTAN at NSU for the usage of experimental equipment.

References

1. K. P. Gopinath, D.-V. N. Vo, D. Gnana Prakash, A. Adithya Joseph, S. Viswanathan, J. Arun. Environ. Chem. Lett. 19, 557 (2021). Crossref
2. W. Li, R. Fang, Y. Xia, W. Zhang, X. Wang, X. Xia, J. Tu. Batteries & Supercaps. 2, 9 (2019). Crossref
3. O. Erol, I. Uyan, M. Hatip, C. Yilmaz, A. B. Tekinay, M. O. Guler. Nanomedicine. 14, 2433 (2018). Crossref
4. S. Farhat, C. D. Scott. J. Nanosci. Nanotechnol. 6, 1189 (2006). Crossref
5. C. Baddour, C. Briens. Int. J. Chem. React. Eng. 3 (2005). Crossref
6. Y.-W. Yeh, Y. Raitses. Carbon. 105, 490 (2016). Crossref
7. S. Iijima. Nature. 354, 56 (1991). Crossref
8. M. Keidar, I. I. Beilis. J. Appl. Phys. 106, 103304 (2009). Crossref
9. M. Kundrapu, M. Keidar. Phys. Plasmas. 19, 073510 (2012). Crossref
10. N. I. Alekseyev, G. A. Dyuzhev. Tech. Phys. 46, 1247 (2001). Crossref
11. N. I. Alekseyev, G. A. Dyuzhev. Tech. Phys. 47, 634 (2002). Crossref
12. N. I. Alekseyev, G. A. Dyuzhev. Tech. Phys. 50, 1551 (2005). Crossref
13. N. I. Alekseyev, G. A. Dyuzhev. Tech. Phys. 50, 1561 (2005). Crossref
14. H. Murayama, S. Tomonoh, J. M. Alford, M. E. Karpuk. Fuller. Nanotub. Carbon Nanostructures. 12, 1 (2003). Crossref
15. N. Arora, N. N. Sharma. Diam. Relat. Mater. 50, 135 (2014). Crossref
16. J. H. J. Scot, S. A. Majetich. Phys. Rev. B. 52, 12564 (2005). Crossref
17. A. A. Iurchenkova, E. O. Fedorovskaya, P. E. Matochkin, S. Z. Sakhapov, D. V. Smovzh. Int. J Energy Res. 44, 10754 (2020). Crossref
18. A. V. Zaikovskii, S. A. Novopashin. Phys. Status. Solidi A. 214, 1700142 (2017). Crossref
19. Z. Wang, N. Li, Z. Shi, Z. Gu. Nanotechnology. 21, 175602 (2010). Crossref
20. K. S. Subrahmanyam, L. S. Panchakarla, A. Govindaraj, C. N. R. Rao. J. Phys. Chem. C. 113, 4257 (2009). Crossref
21. B. Shen, J. Ding, X. Yan, W. Feng, J. Li, Q. Xue. Appl. Surf. Sci. 258, 4523 (2012). Crossref
22. X. Zhao, M. Ohkohchi, H. Shimoyama, Y. Ando. J. Cryst. Growth. 198 –199, 934 (1999). Crossref
23. B. Qin, T. Zhang, H. Chen, Y. Ma. Carbon. 102, 494 (2016). Crossref
24. S. Karmakar, A. B. Nawale, N. P. Lalla, V. G. Sathe, S. K. Kolekar, V. L. Mathe, A. K. Das, S. V. Bhoraskar. Carbon. 55, 209 (2013). Crossref
25. C. Wu, G. Dong, L. Guan. Physica E. 42, 1267 (2010). Crossref
26. B. Li, X. Song, P. Zhang. Carbon. 66, 426 (2014). Crossref
27. V. I. Berezkin. Phys. Status. Solidi B. 226, 271 (2001). Crossref
28. D. V. Smovzh, I. A. Kostogrud, S. Z. Sakhapov, A. V. Zaikovskii, S. A. Novopashin. Carbon. 112, 97 (2017). Crossref
29. Y. Yamaguchi, S. Maruyama. Chem. Phys. Lett. 286, 336 (1998). Crossref
30. S. Usuba, H. Yokoi. J. Appl. Phys. 91, 10051 (2002). Crossref
31. A. V. Krestinin, A. P. Moravsky. Chem. Phys. Lett. 286, 479 (1998). Crossref